Model Order Reduction of Magnetoquasistatic Problems Based on POD and Arnoldi-based Krylov Methods

A. Pierquin[1], T. Henneron[2], S. Clénet[3] and S. Brisset[1]

[1] École Centrale de Lille, L2EP,
Cité Scientifique - CS 20048 - 59651, Villeneuve d'Ascq, France.
[2] Université de Lille, L2EP, Villeneuve d'Ascq, France
e-mail: thomas.henneron@univ-lille1.fr
[3] Arts et Métiers ParisTech, L2EP, Lille, France

The Proper Orthogonal Decomposition method and the Arnoldi-based Krylov projection method are investigated in order to reduce a finite element model of a quasistatic problem. Both methods are compared on an academic example in terms of computation time and precision.

Index Terms—**Krylov subspace, Model Order Reduction, Proper Orthogonal Decomposition, Quasi-static problem.**

I. INTRODUCTION

TO analyse electromagnetic devices, the Finite Element Method (FEM) associated with a time-stepping scheme is often used to solve Maxwell's equations. The discretisation of the space and time domains can yield a large-scale equation system which computation can be dramatically prohibitive when a fine mesh and a high number of time steps are used. To tackle this issue, model order reduction approaches can be investigated. These approaches enable to reduce the size of the problem to solve. In the literature, the Proper Orthogonal Decomposition (POD) [1] and the Arnoldi-based Krylov projection (AKP) [2] approaches have been used to solve many problems in engineering. Both methods consist in performing a projection of the solution onto a reduced basis. For the POD approach, the projector is calculated from a set of solutions of the problem (the snapshots) [3]. For the AKP approach, the projector is deduced from a Krylov subspace built from the equation system to solve in the frequency domain. In computational electromagnetics, the POD method has been already applied to study magnetoquasistatic and electroquasistatic problems [4], [5]. The AKP approach has been used to solve magnetoharmonic problem using the partial element equivalent circuit (PEEC) method [6]. To the author's knowledge, any linear electromagnetic problem hasn't been solved in the time domain using the projector constructed from AKP method in the frequency domain.

In this paper, we propose to apply and compare the POD and AKP methods in the case of quasistatic problems solved by the vector potential formulation in the time domain and the frequency domain. First, the numerical model deduced from the vector formulation is presented. Second, the POD and the AKP methods are described. Finally, an eddy current problem in time and frequency domains is studied by the proposed reduction approaches. The results obtained with reduced models are compared with those deduced from the full model. The two model order reduction methods are also compared in terms of accuracy, computation time and complexity.

II. LINEAR MAGNETOQUASISTATIC PROBLEM

Let us consider a domain Ω of boundary $\Gamma = \Gamma_H \cup \Gamma_B$, $\Gamma_H \cap \Gamma_B = \emptyset$, with a stranded inductor Ω_s and a conducting subdomain Ω_c of boundary $\Gamma_c = \Gamma_E \cup \Gamma_{Jed}$, with $\Gamma_E \subset \Gamma_B$ (Fig. 1). The problem is solved for $\boldsymbol{x} \in \Omega$ and for t in the time interval $[0, T]$.
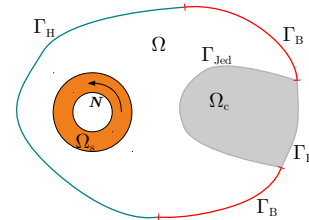

Fig. 1. Spatial domain of the problem.

A magnetoquasistatic problem can be solved by using the vector potential formulation. The potential $\boldsymbol{A}_\star$ is defined such that $\boldsymbol{B}(\boldsymbol{x}, t) = \mathbf{curl}\boldsymbol{A}_\star(\boldsymbol{x}, t)$, $\boldsymbol{E}(\boldsymbol{x}, t) = -\dfrac{\partial \boldsymbol{A}_\star(\boldsymbol{x}, t)}{\partial t}$ and $\boldsymbol{A}_\star(\boldsymbol{x}, t) \times \boldsymbol{n} = 0$ on Γ_B and Γ_E where $\boldsymbol{B}$ is the magnetic flux density and $\boldsymbol{E}$ the electric field. These expressions are combined with Ampère's equation in order to obtain the strong formulation

$$\mathbf{curl}\frac{1}{\mu}\mathbf{curl}\boldsymbol{A}_\star(\boldsymbol{x}, t) + \sigma\frac{\partial \boldsymbol{A}_\star}{\partial t} = \boldsymbol{N}(\boldsymbol{x})i(t), \qquad (1)$$

with μ the magnetic permeability, σ the electric conductivity, $\boldsymbol{N}$ the unit current density vector in Ω_s and i the current flowing through the stranded inductor.

To solve this problem, the potential $\boldsymbol{A}_\star$ is discretized using edge elements and $\boldsymbol{N}$ using facet elements. Applying the Galerkin method to (1), a system of ordinary differential equations is obtained:

$$\boldsymbol{M}\frac{\mathrm{d}\boldsymbol{X}(t)}{\mathrm{dt}} + \boldsymbol{K}\boldsymbol{X}(t) = \boldsymbol{F}i(t). \qquad (2)$$

The vector of unknowns $\boldsymbol{X}(t)$ is composed of the circulations of $\boldsymbol{A}_\star$ along all edges of the mesh, $\boldsymbol{X}(t) = [A_1(t), \ldots, A_{N_{\mathrm{un}}}(t)]^T$. In the case of a sinusoidal supply of frequency f, the problem can be solved in the frequency domain to determine the steady state. Then, the problem is solved for $\boldsymbol{x} \in \Omega$ and for $f \in [f_{min}, f_{max}]$. In this case, (2) becomes

$$(\boldsymbol{M}\mathbf{j}\omega + \boldsymbol{K})\boldsymbol{X}(\omega) = \boldsymbol{F}i(\omega) \tag{3}$$

with $\mathbf{j}$ the imaginary unit and $\omega = 2\pi f$.

III. Model Order Reduction

The principle of the model order reduction is to obtain from (2) or (3) an equation system of reduced size. An orthonormal reduced basis $\boldsymbol{\Psi}$ is determined to approximate the solution $\boldsymbol{X}$ of the full problem under the form $\boldsymbol{\Psi}\boldsymbol{X}_r$, with $\boldsymbol{X}_r$ the solution of the reduced problem:

$$\boldsymbol{M}_r \frac{\mathrm{d}\boldsymbol{X}_r(t)}{\mathrm{d}t} + \boldsymbol{K}_r\boldsymbol{X}_r(t) = \boldsymbol{F}_r i(t) \tag{4}$$

or

$$(\boldsymbol{M}_r\mathbf{j}\omega + \boldsymbol{K}_r)\boldsymbol{X}_r(\omega) = \boldsymbol{F}_r i(\omega) \tag{5}$$

with $\boldsymbol{M}_r = \boldsymbol{\Psi}^T\boldsymbol{M}\boldsymbol{\Psi}$, $\quad \boldsymbol{K}_r = \boldsymbol{\Psi}^T\boldsymbol{K}\boldsymbol{\Psi}$, $\quad \boldsymbol{F}_r = \boldsymbol{\Psi}^T\boldsymbol{F}$.

The Krylov subspace projection and the POD approach are two different ways to determine the reduced basis $\boldsymbol{\Psi}$.

A. Krylov Projection method

For the AKP approach, the solution of the full model is projected onto a Krylov subspace. To determine this subspace, an expansion of the transfer function of the problem is performed. The Laplace's transform is applied to (2):

$$(\boldsymbol{M}s + \boldsymbol{K})\boldsymbol{X}(s) = \boldsymbol{F}i(s). \tag{6}$$

The transfer function has the following expression (see (6))

$$\boldsymbol{h}(s) = (\boldsymbol{M}s + \boldsymbol{K})^{-1}\boldsymbol{F}. \tag{7}$$

$\boldsymbol{h}$ is approximated by a Padé's expansion at the expansion point $s_{\exp}$

$$\boldsymbol{h}(s) = \sum_{j=0}^{\infty} \boldsymbol{h}_j (s - s_{\exp})^j. \tag{8}$$

The vectors $\boldsymbol{h}_j$ can be expressed as

$$\boldsymbol{h}_j = \left(-(\boldsymbol{M}s_{\exp} + \boldsymbol{K})^{-1}\boldsymbol{M}\right)^j (\boldsymbol{M}s_{\exp} + \boldsymbol{K})^{-1}\boldsymbol{F} \tag{9}$$
$$= \boldsymbol{G}^j\boldsymbol{g},$$

with $\boldsymbol{G} = -(\boldsymbol{M}s_{\exp} + \boldsymbol{K})^{-1}\boldsymbol{M}$ and $\boldsymbol{g} = (\boldsymbol{M}s_{\exp} + \boldsymbol{K})^{-1}\boldsymbol{F}$. The set of vectors $(\boldsymbol{h}_j)_{j=0,N_s-1}$ generates the Krylov subspace $\mathcal{K}_{N_s}(\boldsymbol{G}, \boldsymbol{g}) = \mathrm{span}\{\boldsymbol{g}, \boldsymbol{G}^1\boldsymbol{g}, \boldsymbol{G}^2\boldsymbol{g}, \ldots, \boldsymbol{G}^{N_s-1}\boldsymbol{g}\}$. The Arnoldi's algorithm is used to obtain an orthonormal basis $\boldsymbol{\Psi}$ of the Krylov subspace $\mathcal{K}_{N_s}(\boldsymbol{G}, \boldsymbol{g})$ [7]. Thus, $\boldsymbol{\Psi}$ allows to project the solution $\boldsymbol{X}$ onto $\mathcal{K}_{N_s}(\boldsymbol{G}, \boldsymbol{g})$.

Several expansion points s_k can be used to express (7):

$$\boldsymbol{h}(s) = \sum_{j_k=0}^{\infty} \boldsymbol{h}_{j_k}(s - s_k)^{j_k}, \tag{10}$$

with $\boldsymbol{h}_{j_k} = \left(-(\boldsymbol{M}s_k + \boldsymbol{K})^{-1}\boldsymbol{M}\right)^{j_k} (\boldsymbol{M}s_k + \boldsymbol{K})^{-1}\boldsymbol{F}$. The $\boldsymbol{h}_{j_k}$ vectors associated with each expansion point s_k are so-called point moments. The expansion point s_k will be equal to $2\pi f_k$ or $\mathbf{j}2\pi f_k$ according to the problem [8], [9].

B. Proper Orthogonal Decomposition

With the snapshot POD approach [3], the projector $\boldsymbol{\Psi}$ is defined from a set of solutions of the full model (i.e. snapshots). The problem (2) is solved for the N_s first time-steps to obtain $\boldsymbol{X}(t_i), i = 1, \ldots, N_s$, then these solutions are concatenated in the snapshot matrix $\boldsymbol{S} = [\boldsymbol{X}(t_1), \ldots, \boldsymbol{X}(t_{N_s})]$. In the frequency domain, (3) is solved for N_s different frequencies and the snapshot matrix is defined by $\boldsymbol{S} = [\boldsymbol{X}(\omega_1), \ldots, \boldsymbol{X}(\omega_{N_s})]$. Applying the singular value decomposition to the matrix $\boldsymbol{S}$ gives

$$\boldsymbol{S} = \boldsymbol{V}\boldsymbol{\Sigma}\boldsymbol{W}^T \tag{11}$$

with $\boldsymbol{V}_{N_{\mathrm{un}} \times N_{\mathrm{un}}}$ and $\boldsymbol{W}_{N_s \times N_s}$ orthonormal matrices and $\boldsymbol{\Sigma}_{N_{\mathrm{un}} \times N_s}$ a rectangular diagonal matrix of the singular values. The $\boldsymbol{\Psi}$ basis corresponds to the normalised matrix $\boldsymbol{V}\boldsymbol{\Sigma}$ or $\boldsymbol{S}\boldsymbol{W}$. In practice, it is more efficient to compute $\boldsymbol{W}$ by solving the eigenvalues problem on the correlation matrix $\boldsymbol{C}$ of $\boldsymbol{S}$ because $\boldsymbol{C}$ has a smaller size:

$$\boldsymbol{C} = \frac{1}{N_s}\boldsymbol{S}^T\boldsymbol{S} = \boldsymbol{W}\boldsymbol{\Sigma}^T\boldsymbol{V}^T\boldsymbol{V}\boldsymbol{\Sigma}\boldsymbol{W}^T = \boldsymbol{W}\boldsymbol{\Delta}\boldsymbol{W}^T. \tag{12}$$

Then the columns of $\boldsymbol{S}\boldsymbol{W} = \boldsymbol{V}\boldsymbol{\Sigma}$ are normalised to obtain an orthonormal basis $\boldsymbol{\Psi}$.

IV. Applications

The application example is composed of two conducting plates submitted to a magnetic field created by a stranded inductor. Due to its symmetries, only one eighth of the geometry is modeled (Fig. 2). The two model order reduction methods are applied in time-domain and in frequency-domain. In the time-domain, the stranded inductor is supplied by a current $i(t) = \sin(2\pi5000t)$. In the frequency-domain, a current with a magnitude equal to one is imposed for all frequencies. The results obtained with the reduced models are compared with those deduced from the full model.
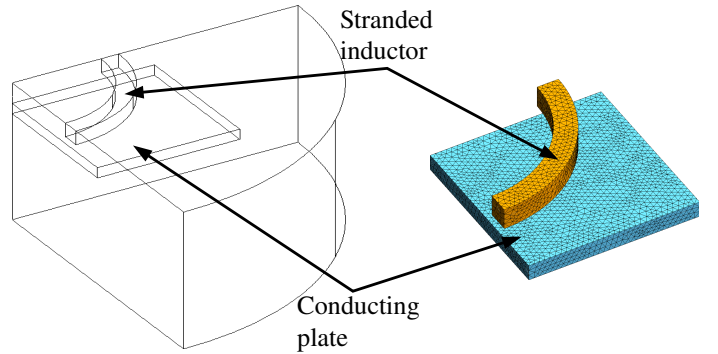

Fig. 2. Geometry and mesh of the device for the stranded inductor and the conducting plate.

A. Quasi static problem

For the quasi static problem in the time domain, the full model (2) is solved by using an implicit Euler scheme. The modeling is performed on 4 periods with 20 points per period. For the POD method, the snapshots are the solutions of the N_s first time steps of the full model. For the AKP approach, only

one expansion point is chosen for the Padé's expansion. The value of the expansion point is equal to the angular velocity of the current: $s_{\text{exp}} = 2\pi 5000$.

In order to evaluate the influence of the size of the reduced basis on a global quantity, the evolutions of the Joule losses versus time, obtained from the POD and AKP models, are compared with the one of the full model in Fig. 3 and Fig. 4. We can observe that the Joule losses converge towards the reference with both approaches when the size of the reduced basis increases. Figures 5(a) and 5(b) present in logscale the error on the Joule losses and on the magnetic energy, $\varepsilon_P = \dfrac{\|P_{\text{ref}} - P_{\text{red}}\|}{\|P_{\text{ref}}\|}$ and $\varepsilon_E = \dfrac{\|E_{\text{ref}} - E_{\text{red}}\|}{\|E_{\text{ref}}\|}$ with P_{ref} and P_{red} (resp. E_{ref} and E_{red}) the evolution of the Joule losses (resp. magnetic energy) obtained from the full and reduced models. For a given size of the reduced basis, the error obtained with the AKP method is smaller than the error obtained with the POD model. Nevertheless, both approaches give the same error when the size of the reduced basis is higher than 12. Figure 6(a) presents the distribution of the eddy current density at a given time step in a cross section of the conducting plate obtained from the full model. Figures 6(b) and 6(c) present the norm of the difference between the eddy current density from the full model and those deduced from the POD and AKP models. The error density is smaller with the AKP method, but considering the scale, the error of the POD model remains acceptable. Figure 7 presents the computation time of the reduced models with respect to the reduced basis size. For both approaches, the computation time is smaller than the one required for the full model. The POD model is faster than the AKP model. This difference comes from the worse matrix conditioning obtained with the AKP method. In fact, with the POD method, due to the Euler scheme, the matrix to inverse is $(M\frac{1}{dt} + K)$, and with the AKP approach, the matrix to inverse is $(Ms_{\text{exp}} + K)$. The profile of the two matrices is the same, but the values of $\frac{1}{dt}$ and s_{exp} are not equal in both cases, that changes consequently the matrix conditioning, and then changes the convergence of the biconjugate gradient (BiCG) used to solve the system. The convergence of BiCG is longer in the case of AKP.

For non linear systems, the POD method can be applied in the same way as in linear case. Recently, the POD method has been associated with the Discrete Empirical Interpolation Method to speed up the accounting of the non linearity with the POD. For electromagnetic problem, this kind of approach has been used to study a single phase transformer [10]. However, the AKP method can not be used directly but the nonlinear behaviour can be taken into account by linearization [11].

B. Magnetoharmonic problem

For the magnetoharmonic problem, we consider a frequency interval from 100 Hz to 20 kHz with a frequency step equal to 100 Hz. For this case, we choose snapshots and expansion points uniformly distributed on the frequency interval. The reduced basis size is fixed at 6. For the POD approach, six snapshots are uniformly distributed on the frequency spectrum. For the AKP method, 3 expansion points are chosen (at 100 Hz, 10 kHz and 20 kHz) and for each expansion point the
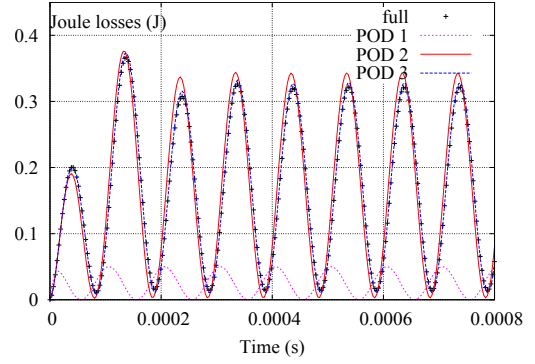

Fig. 3. Evolution of the Joule losses obtained from the POD model with 1,2 and 3 snapshots.
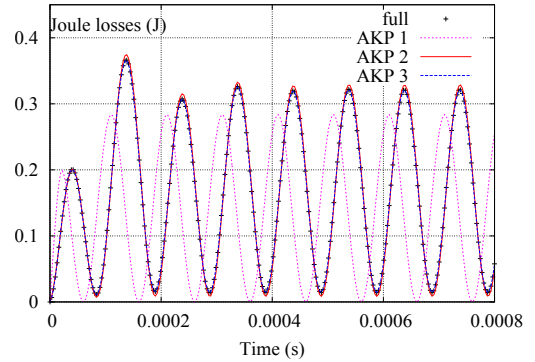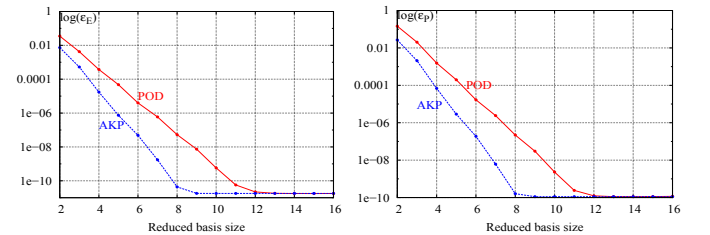

Fig. 4. Evolution of the Joule losses obtained from the AKP model with 1,2 and 3 vectors in $\mathcal{K}_{N_s}(\boldsymbol{G}, \boldsymbol{g})$.

(a) Error on the Joule Losses.

(b) Error on the Magnetic energy.

Fig. 5. Error with respect to the reduced basis size.

two first moments are computed in order to obtain the same size for the two reduced models. Table I presents the error on the magnetic energy and on the Joule losses introduced by the reduced models. For this example, the errors of both reduced models are in a same range. Figure 8(a) presents the real part of the distribution of the eddy current density in a cross section of the conducting plate obtained from the full model. Figures 8(b) and 8(c) present the difference between the real part of the eddy current density from the full model and those deduced from the POD and AKP models. As for the first study in the time domain, the error density is smaller with the AKP method. We can also observe that the eddy current density obtained from both reduced models are close to the one deduced from the full model. The computation time of the reduced models are similar; 199s for the POD approach and 208s for the AKP method. The full model requires 1907s
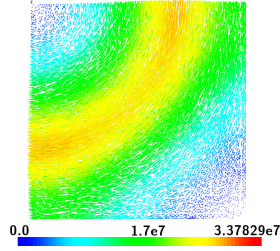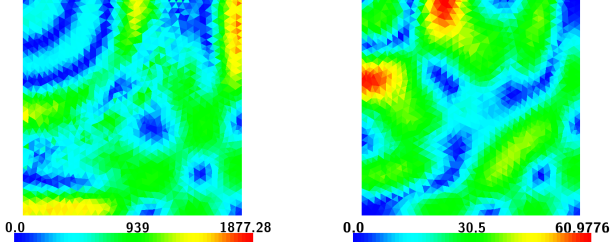
(a) Eddy current density $(\mathrm{A.m^{-2}})$ obtained with full model.

(b) Error density $\|\boldsymbol{J}_{ed}^{\mathrm{full}} - \boldsymbol{J}_{ed}^{\mathrm{POD}}\|$. (c) Error density $\|\boldsymbol{J}_{ed}^{\mathrm{full}} - \boldsymbol{J}_{ed}^{\mathrm{AKP}}\|$.

Fig. 6. Eddy current density of the full model and error density for a reduced basis of size 8, in the conducting plate viewed from the top.
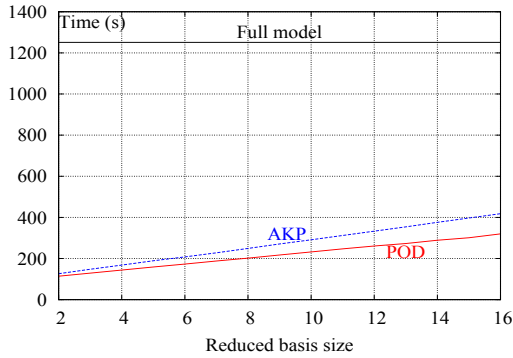

Fig. 7. Computation time with respect to the reduced basis size.

to compute the solution on the frequency interval. Then, the speed up is greater than 9.

TABLE I
ERROR ON MAGNETIC ENERGY AND JOULE LOSSES FOR REDUCED
MODELS OF SIZE 6.

Reduced model	POD	Krylov-Arnoldi
$\dfrac{\|E_{\mathrm{ref}} - E_{\mathrm{red}}\|}{\|E_{\mathrm{ref}}\|}$	$1,7656.10^{-6}$	$1,7322.10^{-6}$
$\dfrac{\|P_{\mathrm{ref}} - P_{\mathrm{red}}\|}{\|P_{\mathrm{ref}}\|}$	$2,0241.10^{-5}$	$2,3489.10^{-5}$

V. CONCLUSION

The Proper Orthogonal Decomposition method and the Arnoldi-based Krylov projection method combined with a FEM vector potential formulation have been developed in order to solve 3D magnetodynamic and magnetoharmonic problems. For the studied example, it has been shown that the two approaches enable to reduce the computation time significantly. The errors on the global and local quantities
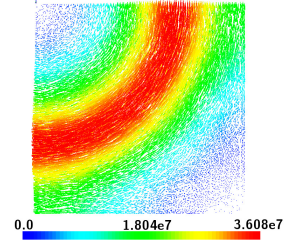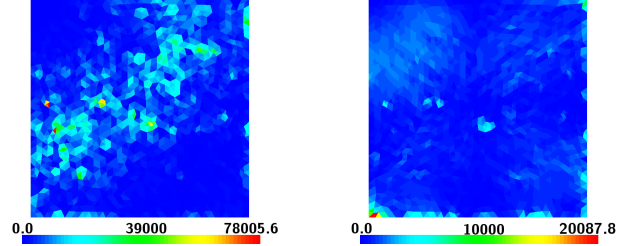

(a) Eddy current density $(\mathrm{A.m^{-2}})$ of the full model.

(b) Error density $\|\boldsymbol{J}_{ed}^{\mathrm{full}} - \boldsymbol{J}_{ed}^{\mathrm{POD}}\|$. (c) Error density $\|\boldsymbol{J}_{ed}^{\mathrm{full}} - \boldsymbol{J}_{ed}^{\mathrm{AKP}}\|$.

Fig. 8. Real part of the eddy current density at 10 kHz and error density, in the conducting plate viewed from the top.

introduced by both reduced models are small compared with the results obtained from the full model. For a given size of the reduced model, the errors associated with the AKP method are smaller than those of the POD approach. Nevertheless, the computation time of the reduced model from the POD method is smaller than this of the AKP approach.

REFERENCES

[1] J. L. Lumley, "The structure of inhomogeneous turbulent flows," in *Atmospheric turbulence and radio propagation* (A. M. Yaglom and V. I. Tatarski, eds.), Moscow: Nauka, 1967.
[2] T. Wittig, I. Munteanu, R. Schuhmann, and T. Weiland, "Two-step lanczos algorithm for model order reduction," *Magnetics, IEEE Transactions on*, vol. 38, pp. 673-676, Mar 2002.
[3] L. Sirovich, "Turbulence and the dynamics of coherent structures, part I: Coherent structures," *Quarterly of Applied Mathematics*, vol. XLV, no. 3, pp. 561-571, 1987.
[4] T. Henneron and S. Clénet, "Model order reduction of quasi-static problems based on pod and pgd approaches," *The European Physical Journal - Applied Physics*, vol. 64, 11 2013.
[5] D. Schmidthausler, S. Schöps, and M. Clemens, "Reduction of linear subdomains for non-linear electro-quasistatic field simulations," *Magnetics, IEEE Transactions on*, vol. 49, pp. 1669-1672, May 2013.
[6] T. S. Nguyen, J.-M. Guichon, O. Chadebec, G. Meunier, et al., "Equivalent circuit synthesis method for reduced order models of large scale inductive peec circuits," CEFC 2012.
[7] A. Odabasioglu, M. Celik, and L. Pileggi, "Prima: passive reduced-order interconnect macromodeling algorithm," in *Computer-Aided Design, 1997. Digest of Technical Papers., 1997 IEEE/ACM International Conference on*, pp. 58-65, Nov 1997.
[8] P. Feldmann and R. Freund, "Efficient linear circuit analysis by Pade approximation via the lanczos process," *Computer-Aided Design of Integrated Circuits and Systems, IEEE Transactions on*, vol. 14, pp. 639-649, May 1995.
[9] A. Cangellaris, M. Celik, S. Pasha, and L. Zhao, "Electromagnetic model order reduction for system-level modeling," *Microwave Theory and Techniques, IEEE Transactions on*, vol. 47, pp. 840-850, Jun 1999.
[10] T. Henneron and S. Clénet, "Model order reduction of non-linear magnetostatic problems based on POD and DEI methods," *Magnetics, IEEE Transactions on*, vol. 50, pp. 33-36, Feb 2014.
[11] Z. Bai, "Krylov subspace techniques for reduced-order modeling of large-scale dynamical systems," *Applied Numerical Mathematics*, vol. 43, no. 1-2, pp. 9-44, 2002.